

Supplementary materials

Enhanced Electrochemical Performance of CTAB-Assisted Zn-Doped Perovskite NiMnO₃ Nanocrystals on Reduced Graphene Oxide for Supercapacitor and Oxygen Evolution Reactions

Suprimkumar D. Dhas¹, Geunchul Kim¹, Pragati N. Thonge^{1,2}, Amar M. Patil³, Avinash C. Mendhe¹, Rabia Batool¹, Daewon Kim^{1}*

¹Department of Electronic Engineering, Institute for Wearable Convergence Electronics, Kyung Hee University, 1732 Deogyeong-daero, Giheung-gu, Yongin 17104, Republic of Korea

² Department of Botany, Punyashlok Ahilyadevi Holkar, Solapur University, Solapur, Maharashtra 416 004, India

³Energy Conversion Engineering Laboratory, Institute of Regional Innovation (IRI), Hirosaki University, Japan

Experimental Details

Pretreatment of graphene oxide nanoribbons (GONRs):

Upon receiving the purchased GONRs, begin by dispersing the GONRs in a mixture of 20 mL DIW and 20 mL ethanol, to form a homogeneous suspension. This can be achieved by ultrasonication, where the mixture is subjected to ultrasonic waves for a 2 h to ensure thorough dispersion. After ultrasonication, centrifuge the suspension at a high speed, for about 30 min. This step helps to separate the unexfoliated particles and any aggregates from the exfoliated nanoribbons. Carefully decant the supernatant containing the dispersed GONRs and transfer it to a new container. The next step involves the washing process, which is critical for removing any residual solvents, contaminants, or by-products from the synthesis process. Add a fresh portion of the solvent to the GONRs, followed by repeated ultrasonication and centrifugation, as described previously. This washing step should be repeated at least three times to ensure thorough cleaning. Finally, the purified GONRs can be collected by air-drying the suspension, yielding a powder form of graphene oxide nanoribbons ready for further characterization.

Calculation Method:

Mass activity: The values of mass activity (A/g) are calculated from the catalyst loading density m and the measured current density $j(\text{mA}/\text{cm}^2)$ at $\eta=0.35\text{V}$. The mass activity can be calculated as follows:

$$\text{Mass activity} = j/m.$$

Specific activity: The values of Specific Activity (mA/cm^2) are calculated from the BET surface area, S_{BET} (m^2/g) and mass activity.

The mass activity can be calculated as follows:

$$\text{Specific activity} = j/(10mS_{\text{BET}}).$$

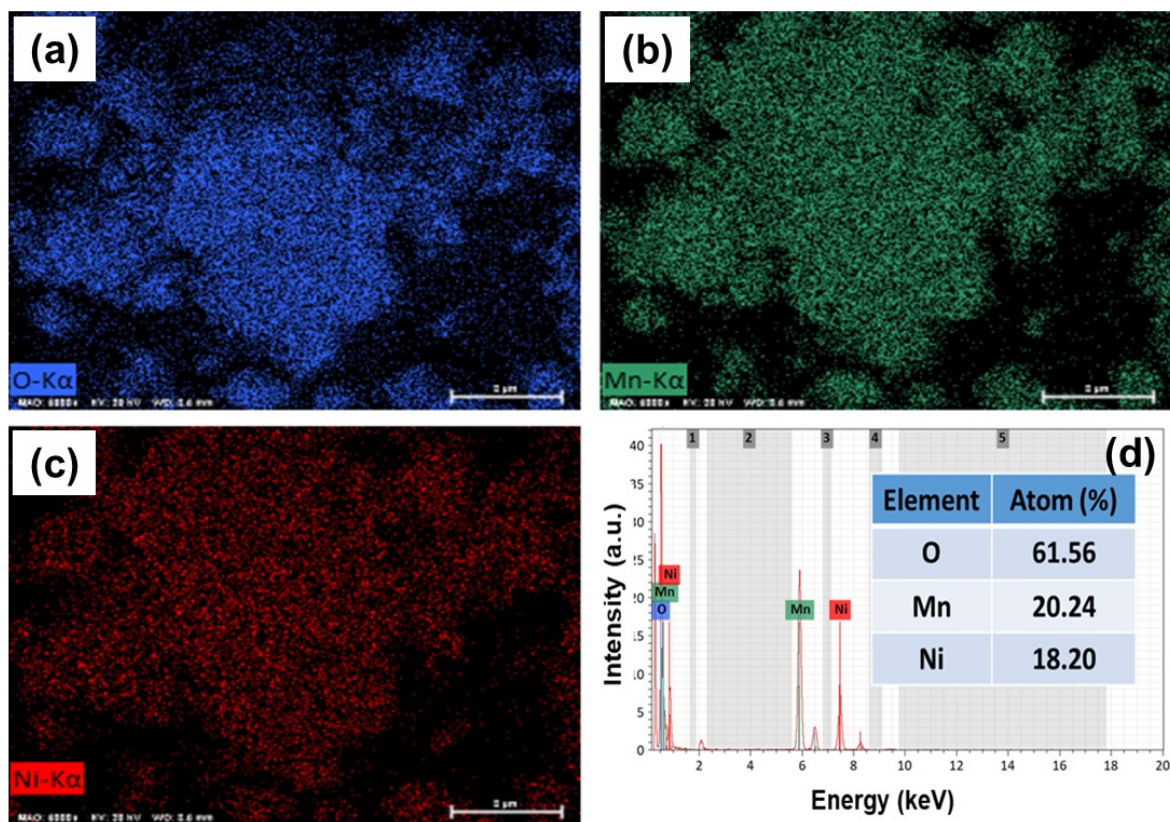


Fig. S1: Element mapping (a) O, (b) Ni, (c) Mn, and corresponding (d) EDS spectra NiMnO₃

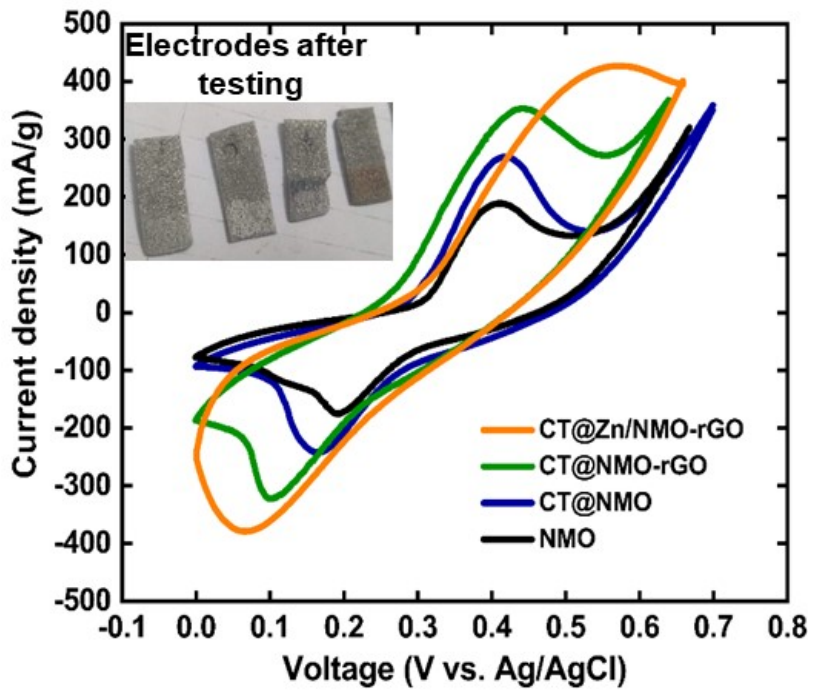


Fig. S2: Comparative CV plot of f NMO based electrodes in 2 M KOH electrolyte (inset actual images of all the electrodes after electrochemical test).

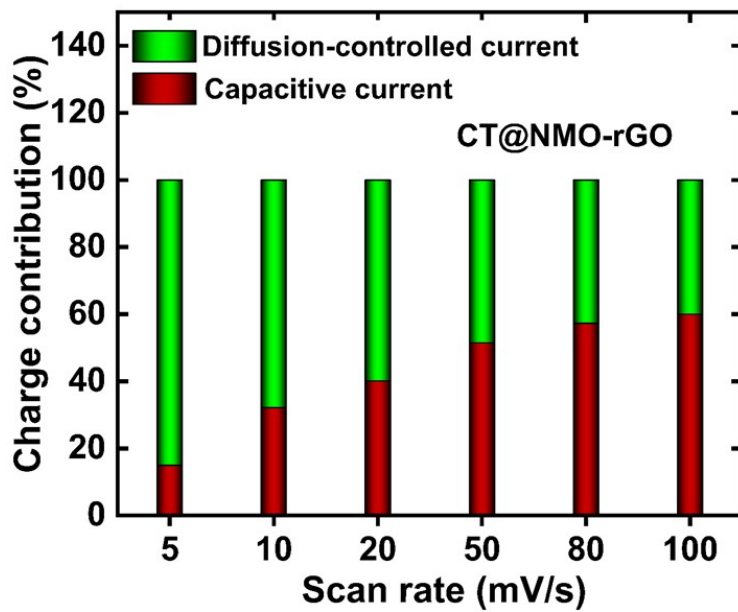


Fig. S3: Capacitive and diffusion-current contributions of CT@NMO-rGO in 2 M KOH electrolyte different scan rates.

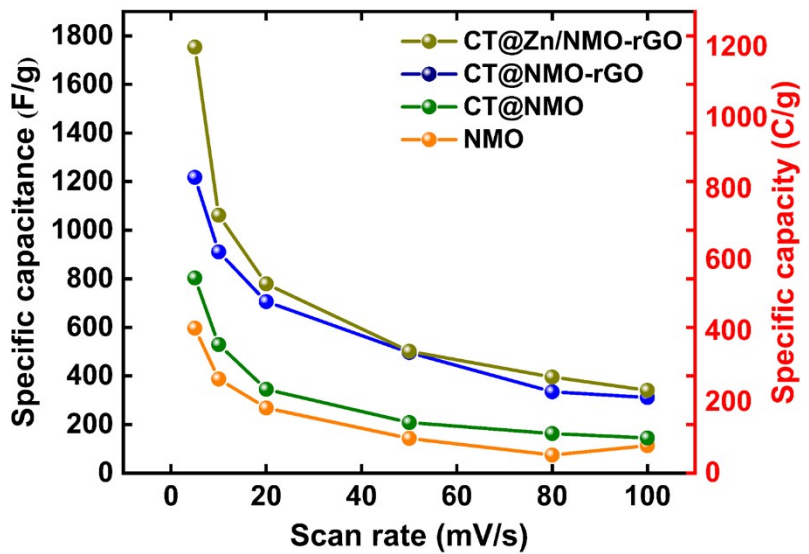


Fig. S4: Plot of specific capacitance/capacity vs scan rate of NMO based electrodes in 2 M KOH electrolyte.

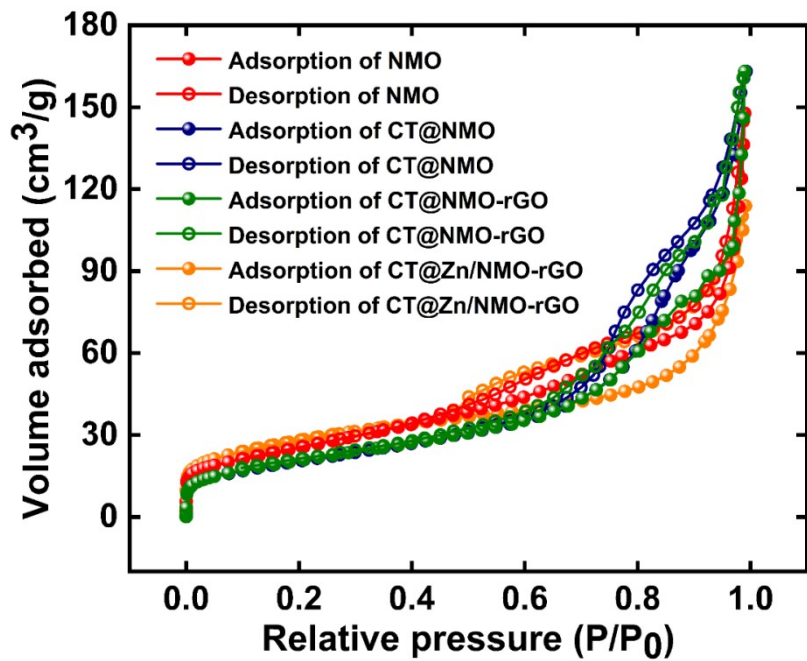


Fig. S5: Comparative N₂ adsorption-deadsorption plot of NMO based electrodes.

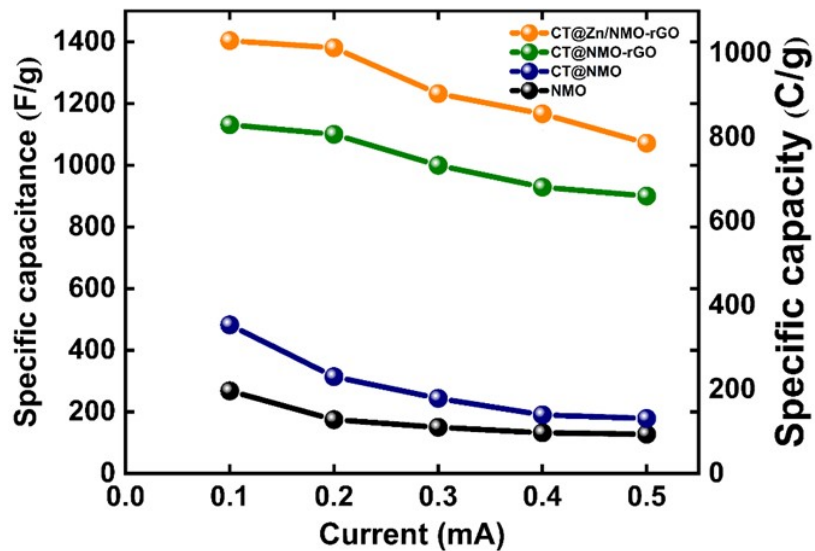


Fig. S6: Plot of specific capacitance/capacity vs current density of NMO based electrodes.

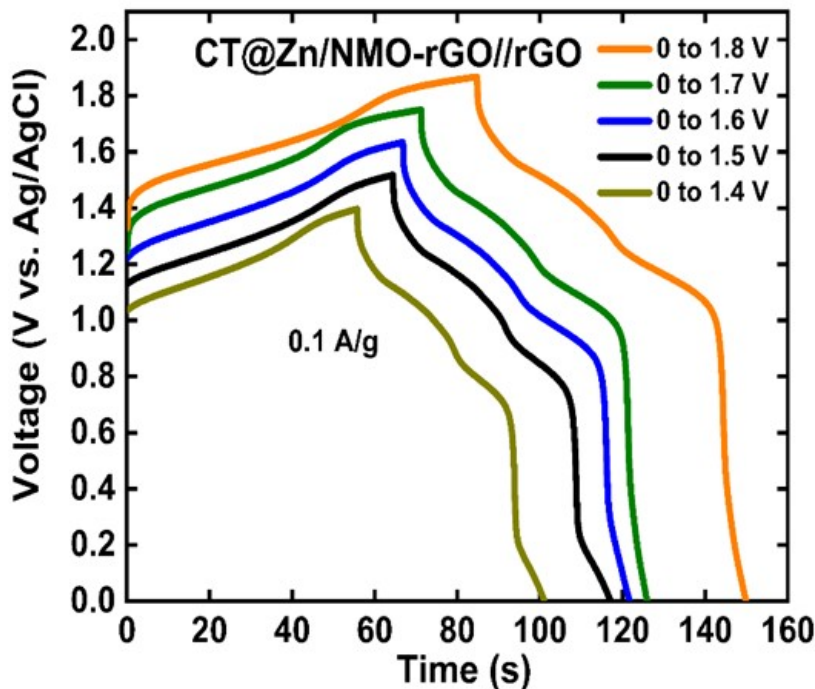


Fig. S7: GCD curves of the CT@Zn/NMO-rGO//AC ASSCS recorded at different potential windows at current density of 0.1 A/g in 2 M KOH electrolyte.

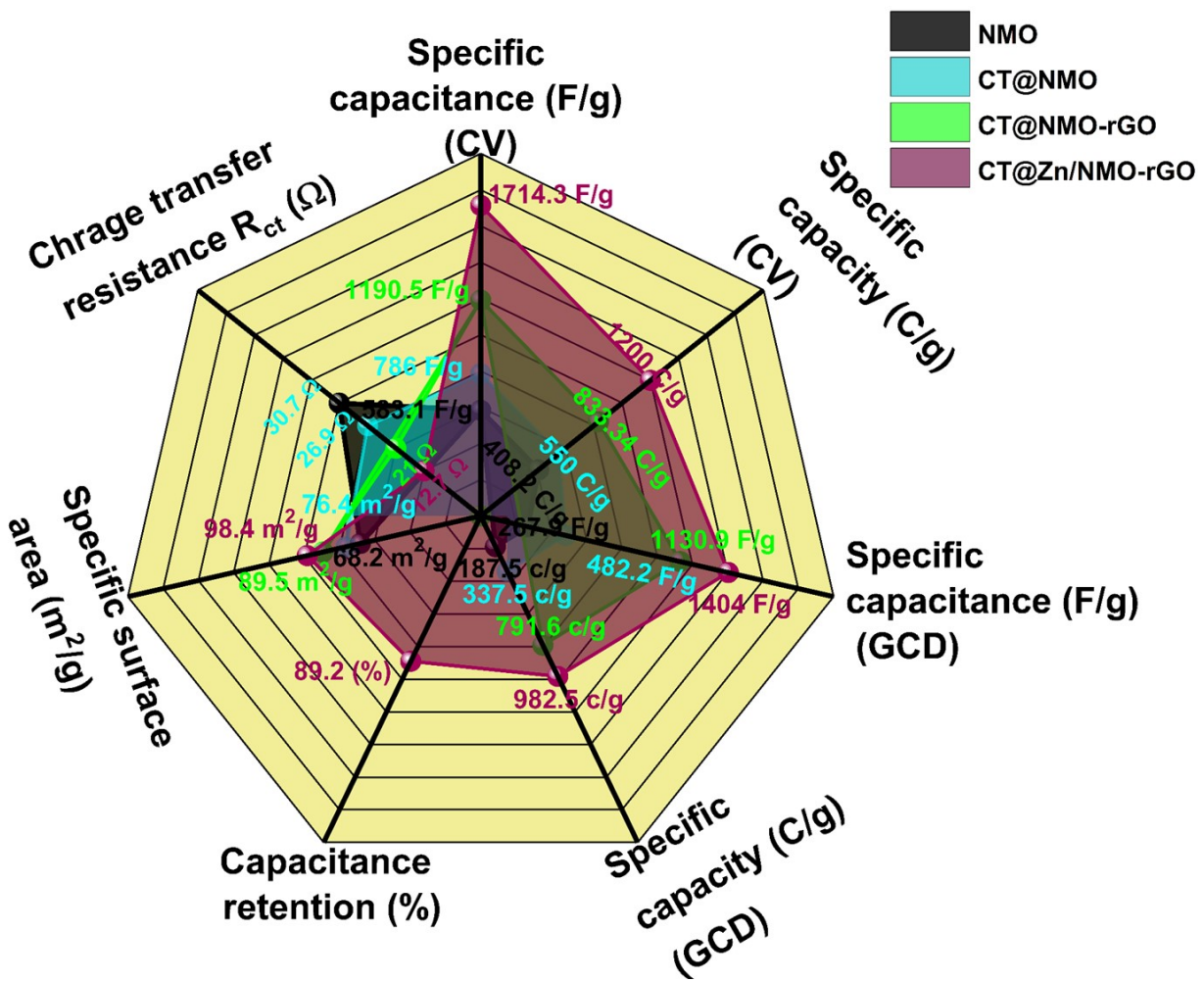


Fig. S8: Radar plot comparison of the performance of the pristine NMO, CT@NMO, CT@NMO-rGO and CT@Zn/NMO-rGO electrodes realized.

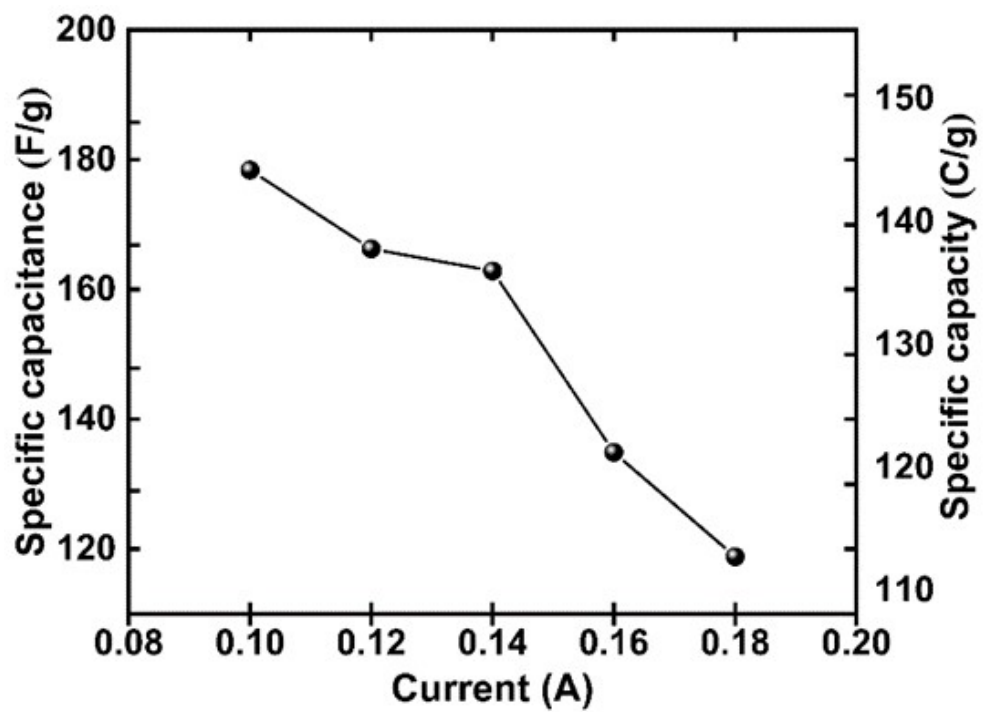


Fig. S9: Plot of specific capacitance/capacity verses current density of CT@Zn/NMO-rGO//AC ASSCS.

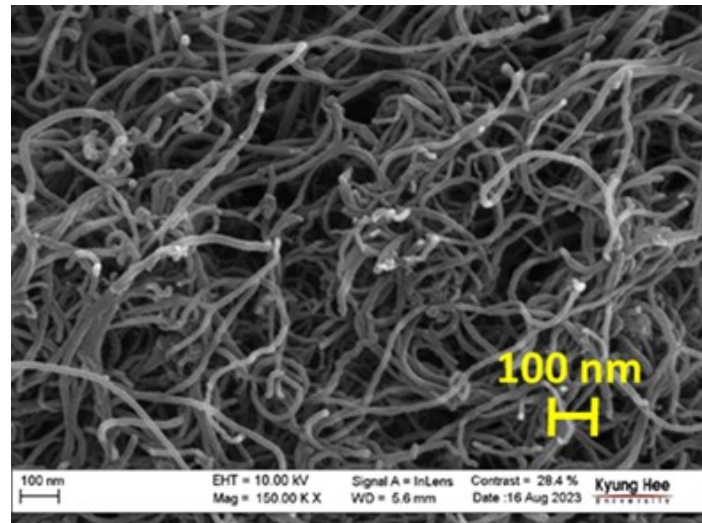


Fig. S10: FE-SEM micrograph of graphene oxide nanoribbon

Sr. No.	Catalyst	Loading density (mg/cm ²)	Overpotential (η) (mV) @10 mA/cm ²	Tafel slope (mV/dec)	Mass activity @η = 0.35 V (A/g)	S _{BET} (m ² /g)	Specific activity @η = 0.35 V (mA/cm ²)
1.	NMO	6.1	465.2	327.3	0.4	68.2	0.005
2.	CT@NMO	6.3	407.1	324.7	0.8	76.4	0.008
3.	CT@NMO-rGO	6.4	352	303.1	1.7	89.5	0.011
4.	RuO ₂	8.1	348.4	268.8	1.72	-	-
5.	CT@Zn/NMO-rGO	9.8	296	144.4	2.54	98.4	0.016
6.	NF	-	549.3	544.5	-	-	-

Table S1: Comparison of OER activity data for NMO-based Catalysts.

Sr. No.	Material	Synthesis Method	Morphology	Current collector	Electrolyte	Specific capacitance Cs (F/g)	Retention % After Cycles	Ref.
1.	Ni _{1-x} Mg _x MnO ₃	Chemical co-precipitation route.	Micro-clusters	NF	6 M KOH	527	89.3/1000	[1]
2.	NiMnO ₃ -rGO-Co ₃ O ₄ /NF	Hydrothermal	Nanoflakes	NF	2 M KOH	3.9 F/cm ²	95.5/5000	[2]
3.	NiMnO ₃	Hydrothermal	Nano-clusters	NF	1 M KOH	435	98.1/2000	[3]
4.	NiMnO ₃	Hydrothermal	Nanocube	NF	6 M KOH	99.03	77/7000	[4]
5.	Fe-doped-NiMnO ₃	Microwave-assisted hydrothermal	Nanoflower	NF	6 mol/L KOH	732.7	78.3/10000	[5]
6.	NiMnO ₃	Hydrothermal	Polycrystalline	Carbon cloth	1 M KOH	230	67/2000	[6]
7.	NiMnO ₃	Microwave-assisted hydrothermal	flower-like nanoballs	NF	6 mol/L KOH	345.8	92/10000	[7]
8.	NiMnO ₃	Electrospinning	Nanosheets	NF	1 M KOH	290	88.6/1000	[8]
9.	NG-NiMnO ₃	Hydrothermal	Rhombohedral	NF	1 M Na ₂ SO ₄	875	88.5/5000	[9]
10.	NiMnO ₃ -rGO	Hydrothermal	Nano-fiber	Cotton-Cu	1 M KOH	404.4 mF/cm ²		[10]
11.	Ni ₆ MnO ₈ / NiMnO ₃	Solvothermal	spheres	NF	6 mol/L KOH	291.9	83.4/5000	[11]
12.	NiMnO ₃ /Ni ₆ MnO ₈	Solvothermal-hydrothermal	nanoblocks@nanoballs	NF	6 M KOH	494.4	88/5000	[12]
13.	Ni/NiMnO ₃ /MnO ₂ @NiMn	Green synthesis	Nanoflakes	NiMn substrate	1 M KOH	2700 F/cm ³		[13]
14.	NiMnO ₃ @NiO	Electrodeposition@ Hydrothermal	Nanospheres@ nanospheres	carbon fiber	4 M KOH	1090	89.6/5000	[14]
15.	NiMnO ₃	Electrodeposition	Nanospheres	carbon fiber	4 M KOH	752	84.2/5000	[14]
16.	NiMnO ₃ /NiMn ₂ O ₄	sol-gel	Nano-cotton	NF	3 M KOH	869		[15]
17.	NiMnO ₃ /NiMn ₂ O ₄ /CNT	Sol-gel auto combustion	Agglomeration-nanoparticled	NF	3 M KOH	1347	67/1000	[15]
18.	NiMnO ₃ -rGO	Hydrothermal	Nanosheets	NF	3 M KOH	91 mA h/g		[16]
19.	NiMnO ₃	Hydrothermal	Nanospheres	NF	3 M KOH	62 mA h/g		[16]
20.	NiMnO ₃	Hydrothermal	Nanosheets	Carbon cloth	6 M KOH	2330 70	67.8/1000	[17]
21.	NiMnO ₃ /GO NiMnO ₃ /rGO	Co-precipitation	Microspheres	NF	0.01 M KOH	170 285	87/1000	[18]
22.	CT@zn/NMO-rGO	Chemical reduction method	Nanoplates	NF	1 M KOH	1404	89.2/30000	This Work

Table S2: Capacitive performance comparison of some nickel, cobalt, manganese based metal oxides and NF based electrodes.

References

- [1] V. Jose, V. Jose, E. Kuruvilla, M. Arunkumar, A. Segar Deepi, G. Srikesh, A. Samson Nesaraj, Facile chemical synthesis of Mg-doped NiMnO₃ perovskite based nanostructured materials: Application in photocatalysis and supercapacitors, Inorganic Chemistry Communications. 156 (2023) 111205. <https://doi.org/10.1016/j.inoche.2023.111205>.
- [2] K.S. Ranjith, S.M. Ghoreishian, N.R. Chodankar, G.S.R. Raju, S.J. Patil, Y.S. Huh, Y.K. Han, Hierarchical layer to layer of ternary heterostructure: Nanograin nickel carbonate embedded layered NiMnO₃-rGO-Co₃O₄ composite array as a high-performance electrode for hybrid supercapacitors, International Journal of Energy Research. 46 (2022) 15066–15080. <https://doi.org/10.1002/er.8206>.
- [3] S.D. Dhas, P.S. Maldar, M.D. Patil, K.M. Hubali, U. V. Shembade, S.B. Abitkar, M.R. Waikar, R.G. Sonkawade, G.L. Agawane, A. V. Moholkar, Hydrothermal synthesis of mesoporous NiMnO₃ nanostructures for supercapacitor application: Effect of electrolyte, Journal of Energy Storage. 35 (2021) 102277. <https://doi.org/10.1016/j.est.2021.102277>.
- [4] H. Kim, J. Shin, I. Jang, Y. Ju, Perovskite NiMnO₃ Oxide and Application in Supercapacitor Electrode, Energies. (2019).
- [5] S. Qiao, N. Huang, J. Zhang, Y. Zhang, Y. Sun, Z. Gao, Microwave - assisted synthesis of Fe - doped NiMnO₃ as electrode material for high - performance supercapacitors, (2024) 1–12.
- [6] M. Dinesh, Y. Haldorai, R.T. Rajendra Kumar, Mn–Ni binary metal oxide for high-performance supercapacitor and electro-catalyst for oxygen evolution reaction, Ceramics

International. 46 (2020) 28006–28012. <https://doi.org/10.1016/j.ceramint.2020.07.295>.

- [7] S. Qiao, N. Huang, Y. Sun, J. Zhang, Y. Zhang, Z. Gao, Microwave-assisted synthesis of novel 3D flower-like NiMnO_3 nanoballs as electrode material for high-performance supercapacitors, Journal of Alloys and Compounds. 775 (2019) 1109–1116. <https://doi.org/10.1016/j.jallcom.2018.10.216>.
- [8] D. Tian, X. Lu, G. Nie, M. Gao, C. Wang, Direct growth of Ni-Mn-O nanosheets on flexible electrospun carbon nanofibers for high performance supercapacitor applications, Inorganic Chemistry Frontiers. 5 (2018) 635–642. <https://doi.org/10.1039/c7qi00696a>.
- [9] S. Giri, D. Ghosh, C.K. Das, One pot synthesis of ilmenite-type NiMnO_3 -“nitrogen-doped” graphene nanocomposite as next generation supercapacitors, Dalton Transactions. 42 (2013) 14361–14364. <https://doi.org/10.1039/c3dt51807h>.
- [10] S.R. Ghorbani, H. Arabi, R. Ghanbari, NiMnO_3 rGO nanocomposites in a cotton - based flexible yarn supercapacitor, (2024) 1–19.
- [11] S. Qiao, S. Zhou, N. Huang, J. Zhang, Y. Sun, L. Yang, X. Du, Novel $\text{Ni}_6\text{MnO}_8/\text{NiMnO}_3$ composite as a highly stable electrode material for supercapacitors, Materials Letters. 255 (2019) 126509. <https://doi.org/10.1016/j.matlet.2019.126509>.
- [12] S. Qiao, N. Huang, Y. Zhang, J. Zhang, Z. Gao, S. Zhou, One-step synthesis of nanoblocks@nanoballs $\text{NiMnO}_3/\text{Ni}_6\text{MnO}_8$ nanocomposites as electrode material for supercapacitors, International Journal of Hydrogen Energy. 44 (2019) 18351–18359. <https://doi.org/10.1016/j.ijhydene.2019.05.108>.
- [13] A. Thomas, A. Kumar, G. Perumal, R.K. Sharma, V. Manivasagam, K. Popat, A.

Ayyagari, A. Yu, S. Tripathi, E. Buck, B. Gwalani, M. Bhogra, H.S. Arora, Oxygen-Vacancy Abundant Nanoporous Ni/ NiMnO₃/MnO₂@NiMn Electrodes with Ultrahigh Capacitance and Energy Density for Supercapacitors, ACS Applied Materials and Interfaces. 15 (2023) 5086–5098. <https://doi.org/10.1021/acsami.2c16818>.

- [14] Y. Chen, L.T. Cao, P. Lian, J.H. Guan, Y. Liu, Preparation and electrochemical properties of NiMnO₃@NiO nanosheets for pseudocapacitors, Journal of Alloys and Compounds. 832 (2020) 154936. <https://doi.org/10.1016/j.jallcom.2020.154936>.
- [15] S. Karmakar, D. Behera, Small polaron hopping conduction in NiMnO₃/NiMn₂O₄ nanocotton and its emerging energy application with MWCNT, Ceramics International. 45 (2019) 13052–13066. <https://doi.org/10.1016/j.ceramint.2019.03.237>.
- [16] J.S. Sanchez, A. Pendashteh, J. Palma, M. Anderson, R. Marcilla, Synthesis and application of NiMnO₃-rGO nanocomposites as electrode materials for hybrid energy storage devices, Applied Surface Science. 460 (2018) 74–83. <https://doi.org/10.1016/j.apsusc.2018.02.165>.
- [17] F. Mu, J. Zhao, C. Gu, Ultrathin porous NiMnO₃ nanosheets on carbon cloth for use as supercapacitor electrode, AIP Advances. 10 (2020). <https://doi.org/10.1063/5.0009246>.
- [18] X. Jiao, X. Xia, G. Zhang, M. Kong, H. Chauhan, M.K. Singh, Synthesis of NiMnO₃/C nano-composite electrode materials for electrochemical capacitors, (n.d.).